Available online at www.sciencedirect.com

ScienceDirect

Ceramics International 40 (2014) 4933–4937

CERAMICS INTERNATIONAL

www.elsevier.com/locate/ceramint

Effect of surfactants on the synthesis of Al_2O_3–CeO_2 nanocomposite using a reverse microemulsion method

Reza Pournajaf[a], S.A. Hassanzadeh-Tabrizi[a,*], M. Ghashang[b]

[a]Young Researchers and Elite Club, Najafabad Branch, Islamic Azad University, Isfahan, Iran
[b]Faculty of Sciences, Department of Chemistry, Najafabad Branch, Islamic Azad University, Isfahan, Iran

Received 24 September 2013; received in revised form 18 October 2013; accepted 18 October 2013
Available online 25 October 2013

Abstract

Al_2O_3–CeO_2 nanocomposite was synthesized by a reverse microemulsion method. Effects of surfactants (Sodium dodecyl sulfate, Cetyltrimethyl ammonium bromide and Polyoxyethylene(23)lauryl ether) on size, morphology and surface area of alumina–ceria nanocomposite were investigated. The synthesized products were studied by X-ray diffraction (XRD), thermogravimetric and differential thermal analysis (DTA–TG), Brunauer–Emmett–Teller surface area measurement (BET), scanning electron microscopy (SEM) and transmission electron microscopy (TEM). XRD revealed that Al_2O_3–CeO_2 nanoparticles with crystallite size in nanometer scale were formed. TEM images showed that the material was composed of nanoparticles with an average size of 20 nm. Properties of the synthesized nanocomposite can be tailored by changing the surfactant.

Keywords: Ceramics; Chemical synthesis; Nanostructures; Transmission electron microscopy

1. Introduction

Alumina is the most widely used catalyst support material in catalytic processes due to its favorable textural properties and mechanical/thermal stability [1]. Its properties such as high specific surface area, surface acidity and defects in its crystalline structures are important factors in a wide range of applications. Nowadays, the alumina–ceria supported system constitutes one of the most widely used mixed-oxides for elimination of pollutants in automobile exhaust gases [2,3]. Ceria (CeO_2), with a cubic fluorite-type structure and one of the most reactive rare earth metal oxides, is used in applications such as catalysis, optical additive, ionic conduction and as counter-electrodes in electrochromic devices [4]. Oxygen vacancy in CeO_2 due to many Ce^{4+}/Ce^{3+} redox sites can be rapidly formed and removed which results in its remarkable oxygen storage capacity [5].

Nanomaterials have generated a lot of interest due to their unique physical and chemical properties that are significantly different from those of bulk materials. Reducing the particles' size to a few nanometers, while keeping its chemical composition fixed, can change the fundamental properties of a material [6]. In a nano-scale form, as particle size decreases, the amount of lattice defects such as oxygen vacancies and grain boundary increases [7]. As known a synthesis route has an important effect on properties of products. Conventional processes for synthesizing ceramic nanopowders involve mechanochemical [8], co-precipitation [9], sol–gel [10], hydrothermal [11] and microemulsion synthesis [12] and other related methods. Among these methods, chemical processes produce fine particles of high purity and high specific surface area. In addition chemical processes achieve intimate mixing of reactant cations on the atomic level, leading to an increase in reaction rate and lowering synthesis temperature.

In recent years, a microemulsion method has been studied and utilized widely and has been a key technique to synthesize oxide nanoparticles owing to the products which have characteristics of good dispersitivity, controlled size and narrow

*Corresponding author. Tel.: +98 3312291111; fax: +98 3312291016.
E-mail addresses: tabrizi1980@gmail.com, hassanzadeh@pmt.iaun.ac.ir (S.A. Hassanzadeh-Tabrizi).

0272-8842/$ - see front matter © 2013 Elsevier Ltd and Techna Group S.r.l. All rights reserved.
http://dx.doi.org/10.1016/j.ceramint.2013.10.086

size distribution. Microemulsions are isotropic and thermodynamically stable solutions containing at least three components, namely a polar phase (usually water), a nonpolar phase (usually oil) and a surfactant. These thermodynamically stable dispersions can be considered as truly nanoreactors which can be used to carry out chemical reactions and, in particular, to synthesize nanomaterials. Reverse microemulsions' technique is one of the most recognized methods due to its several advantages, for instance, soft chemistry, demanding no extreme pressure or temperature control, easy handling, and requiring no special or expensive equipment, and was invented as an effective process for preparing nanoparticles [13].

In the present work for the first time, an alumina–ceria composite nanopowder was synthesized via a water-in-oil microemulsion method by three different kinds of surfactants. Decomposition of the precipitate and effect of surfactants on surface area, morphology and particle size of the synthesized alumina–ceria composite powder were investigated.

2. Experimental procedure

2.1. Materials and method

Aluminum nitrate ($Al(NO_3)_3 \cdot 9H_2O$) and ammonium cerium nitrate ($(NH_4)_2Ce(NO_3)_6$) were used as aluminum and cerium precursors respectively. Cyclohexane as an oil phase, Sodium dodecyl sulfate (SDS) as an anionic surfactant, Cetyltrimethyl ammonium bromide (CTAB) as a cationic surfactant, Polyoxyethylene(23)lauryl ether (BRIJ-35) as an nonionic surfactant and *n*-butyl alcohol as a cosurfactant were used. All chemicals were of analytical grade and used without further purification (Merck Co.).

Two types of microemulsion solutions were prepared in advance. In the first solution, metal salts aqueous solution (Al/Ce mol ratio = 10/0.5) was added drop-wise into the mixture of cyclohexane/surfactant/*n*-butyl alcohol under magnetic stirring. After continuous stirring for 30 min, a homogenous and transparent solution was obtained. The second microemulsion solution was made in the same manner except that the metal salts aqueous solution was replaced by NH_4OH solution. The two obtained optically transparent solutions were mixed and stirred for 1 h to form a precipitate (pH = 9). The precipitate was collected by centrifuging and washed with ethanol. The precursor powders were dried at 80 °C for 1 h and then calcined at 800 °C for 2 h. The flow chart of the powder preparation is shown in Fig. 1.

2.2. Characterization

X-ray diffraction (XRD) measurements of the prepared samples were performed using a Philips X'pert model with CuKα radiation. The crystallite size (*d*) of the powder was measured from the Scherrer equation. Differential thermal analysis (DTA) and thermogravimetry (TG) were used in the range of 25–950 °C with a rate of 10 °C/min with an STA

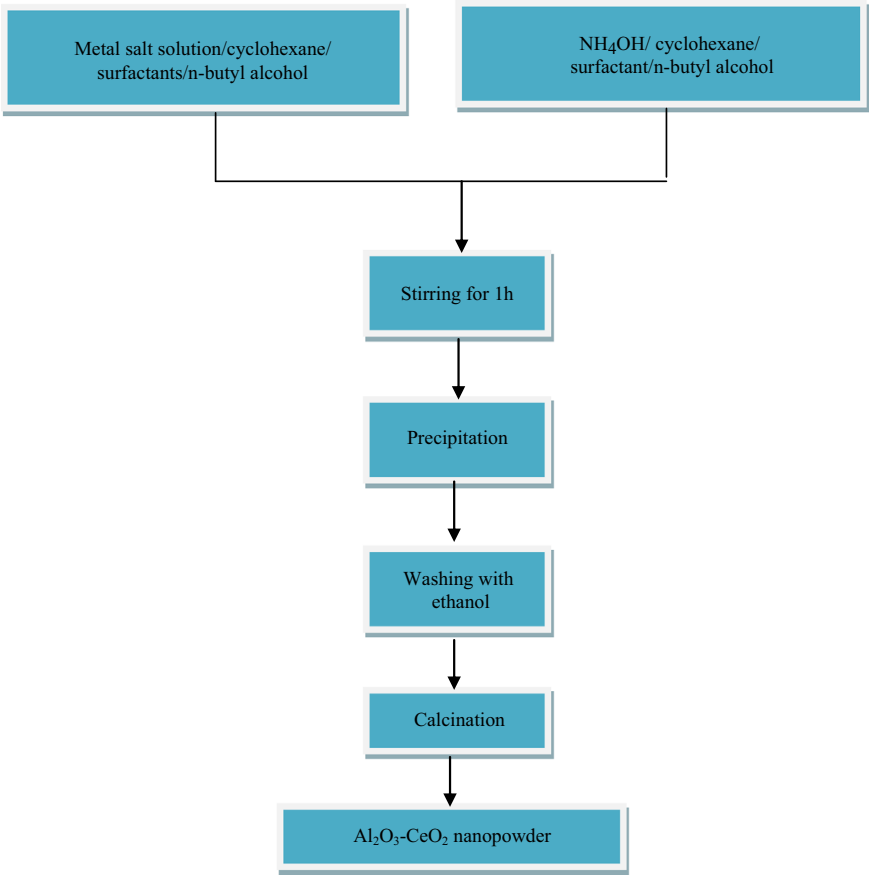

Fig. 1. Flow chart of reverse microemulsion processing.

equipment (STA 1640). The BET specific surface area was determined by nitrogen adsorption at 77 K using a Sorptometer Kelvin1042 surface area and porosimetry analyzer, operating in a single point mode. The morphology of prepared samples was investigated by using a field emission scanning electron microscope (FE-SEM). TEM electron micrograph of the powders was recorded with a JEM-100CX transmission electron microscope.

3. Results and discussion

Fig. 2 presents thermogravimetry and differential thermal analysis (TG–DTA) curves of the dried precipitated powder in air atmosphere. In the first stage, according to the TG curve, a mass loss of about 16.77% at around 80–238 °C was observed and in the DTA curve, two low intensity endothermic peaks at 108 and 220 °C were observed, which are attributed to the loss of adsorbed water and dehydration of precipitate. In the second step at 238 °C, the precursor shows rapid and sudden mass loss of about 28% and an exothermic peak associated with burning and removal of residual surfactant, co-surfactant and cyclohexane in the sample. Two exothermic peaks at 300 and 425 °C and mass loss of approximately 22.21% are attributed to removal of volatile groups such as nitride group and oxidation of cerium and aluminum components. No significant weight loss occurs after 500 °C. The total weight loss of 67.22% appears in the precipitate.

The X-ray diffraction patterns of the samples heat treated at 800 °C are shown in Fig. 3. In all three patterns, γ-alumina and ceria peaks were observed but in the sample prepared by SDS, the peaks have high intensity which is due to further crystal growth. In the other two patterns the peaks are wide and have low intensity. The sample prepared by CTAB shows wider peaks than that of the sample prepared by BRIJ-35 which is due to lower growth of crystallites in this sample. XRD crystallite size of the samples (d) can be estimated from XRD patterns by substituting the value of the full-width at half maximum (FWHM) of broadened characteristic peaks to Scherrer's equation as follows:

$$d = \frac{0.9\lambda}{\mathrm{FWHM}\ \cos\ (\theta)} \quad (1)$$

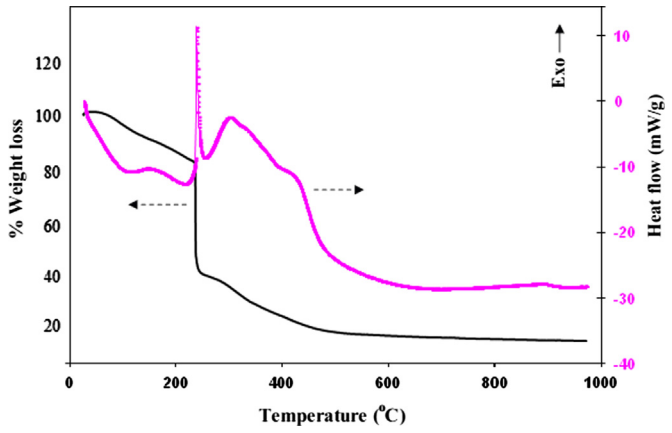

Fig. 2. DTA and TG curves of the samples.

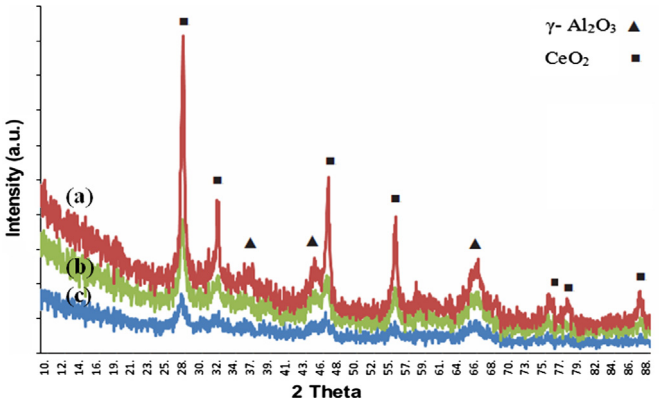

Fig. 3. XRD patterns of composite samples heat treated at 800 °C for 2 h: (a) SDS, (b) BRIJ-35, and (c) CTAB.

where λ is the X-ray wavelength and θ is the diffraction angle for the plane. The average crystallite size of samples with different surfactants is shown in Fig. 4. The crystallite size of the sample prepared by CTAB (about 7 nm) is smaller than that of other samples (about 10 and 20 nm for BRIJ-35 and SDS, respectively). It seems that CTAB is a more effective surfactant than the others for inhibiting crystal growth. The smaller crystallite size derived from CTAB surfactant may be attributed to the fact that the nucleation and subsequent growth of particles took place in a controlled manner on the smaller droplets of water phase, which were dispersed in a continuous oil phase with CTAB molecules residing at the interface.

Although the preparation of the Al_2O_3–CeO_2 composite has been studied before, not much information is available on the influence of surfactants on the surface area of Al_2O_3–CeO_2 composite. This is very important since this composite would be used for a variety of applications such as automotive catalysts [14]. Therefore, in this study the effect of surfactant on the surface area was also investigated (Fig. 5). The surface areas of powders prepared by CTAB, BRIJ-35 and SDS were 162, 134 and 120 m^2/g, respectively. As can be seen, the highest surface area was obtained for the sample prepared by CTAB. As known, most of the surfactant molecules consisted of two tails: one is the hydrophobic head group, and the other is the hydrophilic head group [15]. These molecules are inserted into the particle layer. Finally, molecules are removed by calcination, so many pores are obtained on the surface of particles which result in increase of surface area [16]. Higher surface area of the sample with CTAB may be attributed to the higher degree of incorporation of this surfactant at the surface of nanoparticles. According to Figs. 4 and 5, it can be concluded that the unique synthesis process of microemulsion method brought an improvement in the manipulation of crystallite size and surface area of the materials.

The SEM micrographs of prepared samples calcined at 800 °C are shown in Fig. 6. As can be seen, powders consist of some agglomerates which are due to the ultrafine size of particles and their high surface area. By increasing the temperature during calcination, the mechanism that can be activated is surface diffusion, which leads to neck formation and further agglomeration. Particle size of the sample prepared

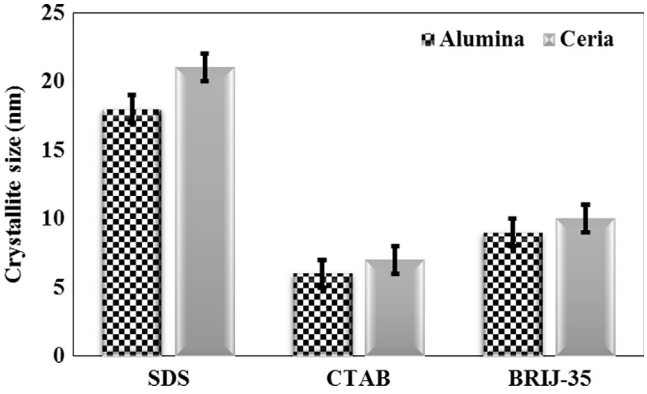

Fig. 4. Crystallite sizes of samples prepared by different surfactants.

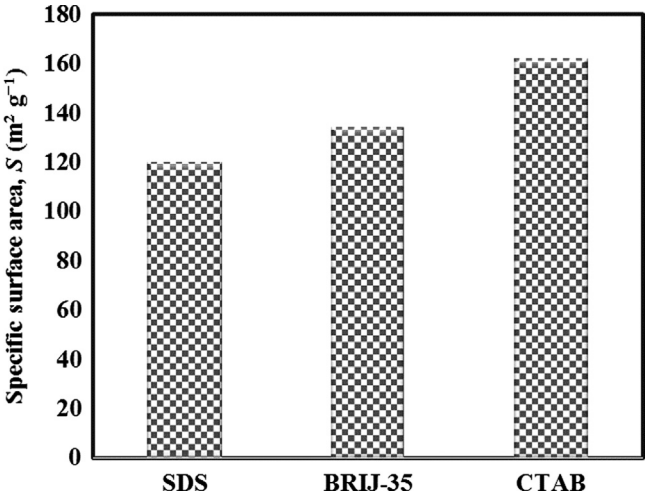

Fig. 5. Surface area of composite samples prepared by different surfactants and calcined at 800 °C.

by SDS is higher than that of other samples. For better determination of size and morphology of the powders, a transmission electron microscope was used for the samples prepared by BRIJ-35 and CTAB (Fig. 7). The TEM images confirm that the agglomerates comprise connected smaller crystalline nanoparticles. In addition, particles with sizes of about 20 nm in the sample prepared by CTAB are shown which are smaller than particles prepared with the addition of BRIJ-35. This is consistent with the crystallite sizes calculated by XRD results as shown in Fig. 4. As known, in this method, particles are formed in the internal structure of the microemulsion, which is determined by the ratio of water to surfactant. At high oil concentration, the bicontinuous phase is transformed into a structure of small water droplets within a continuous oil phase when surfactant is added. Therefore the size of droplets determines the particle size, depending on the kind and amount of surfactant [17]. Surfactants play two important roles in the microemulsion synthesis. First, the addition of surfactant enhances the emulsification in the system, which facilitates the homogenous mixing of the raw materials. Second, surfactant could also inhibit the excess aggregation of particles because the surfactant could be absorbed on the surface of the particles [18]. It seems that absorbance of CTAB on the

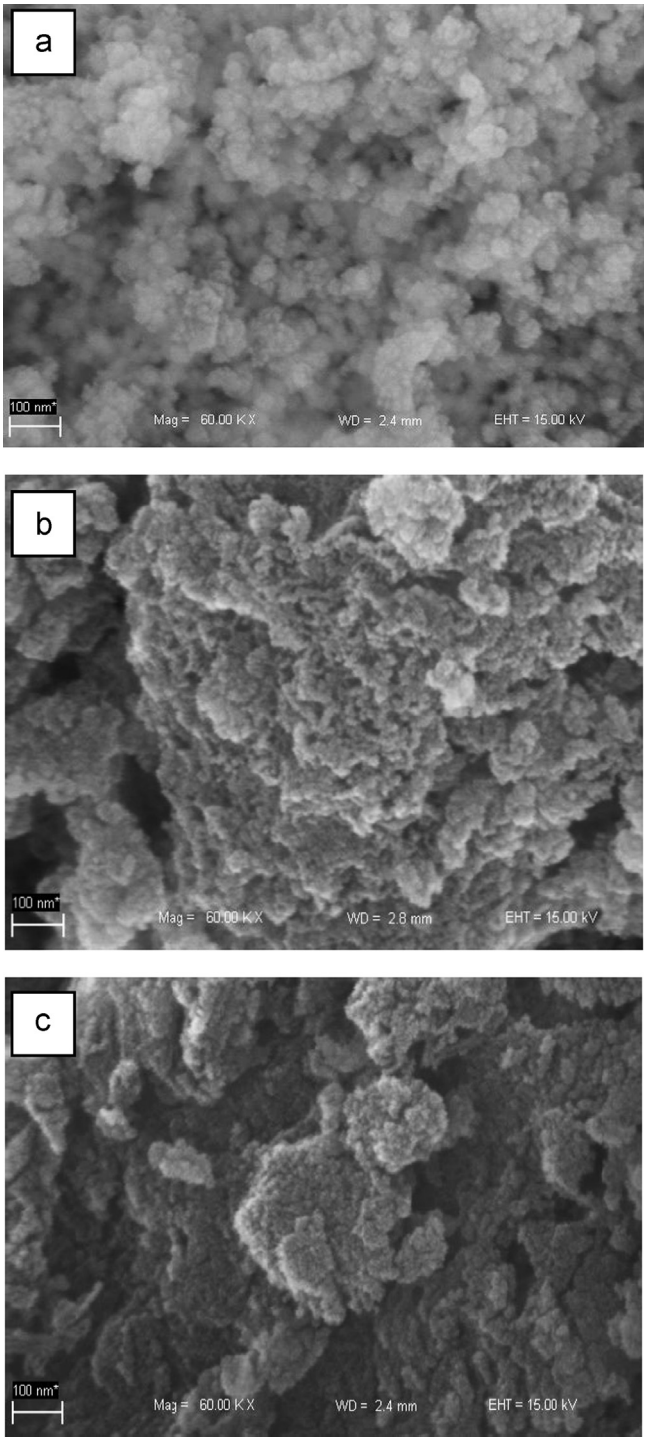

Fig. 6. SEM images of samples heat treated at 800 °C and prepared by different surfactants: (a) SDS, (b) BRIJ-35, and (c) CTAB.

surface of particles is more than that of other surfactants which results in smaller particles.

4. Conclusion

In this paper, Al_2O_3–CeO_2 nanocomposite was prepared by a reverse microemulsion method with aluminum nitrate and ammonium cerium nitrate as precursors. The results showed

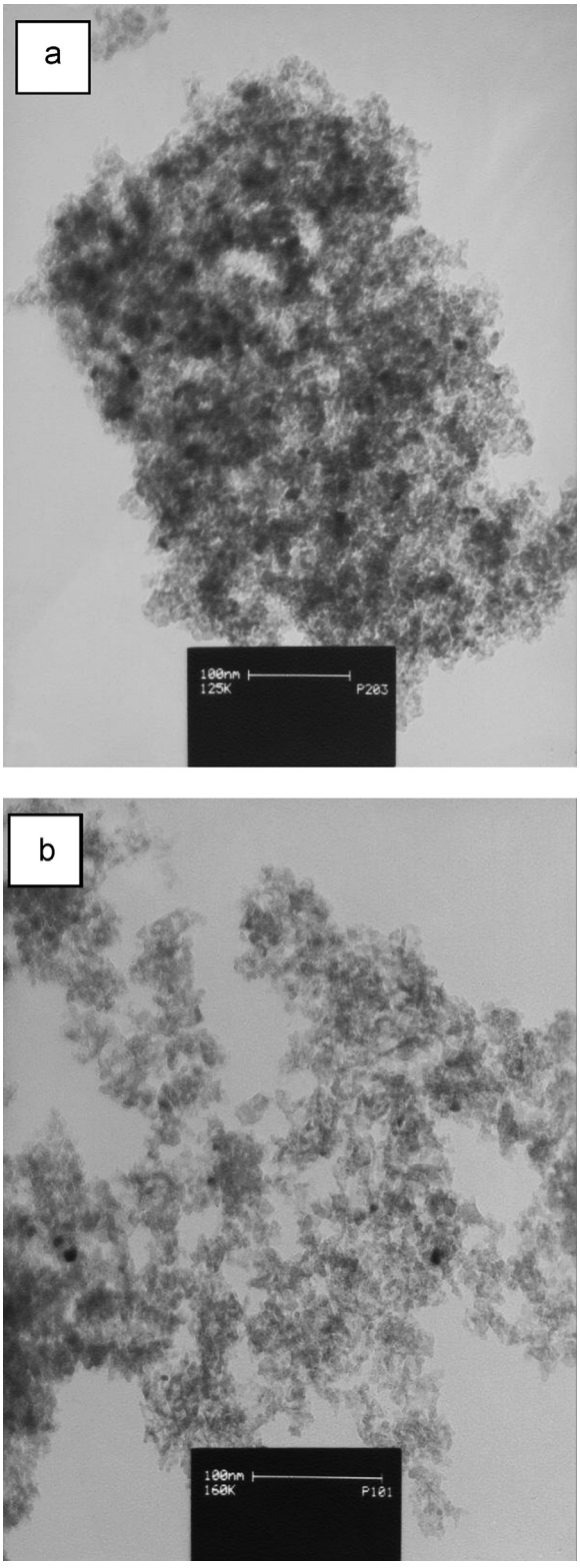

Fig. 7. TEM images of samples heat treated at 800 °C and prepared by (a) BRIJ-35 and (b) CTAB.

that the kind of surfactant has an important effect on the size, morphology and surface area of the products. XRD results revealed that Al_2O_3–CeO_2 nanoparticles with crystallite size in nanometer scale were formed. Nanoparticles prepared by CTAB were smaller, with higher surface area than those of particles prepared by BRIJ-35 and SDS.

References

[1] B. Huang, C.H. Bartholomew, S.J. Smith, B.F. Woodfield, Facile solvent-deficient synthesis of mesoporous γ-alumina with controlled pore structures, Microporous Mesoporous Mater. 165 (2013) 70–78.
[2] S.A. Hassanzadeh-Tabrizi, E. Taheri-Nassaj, Sol–gel synthesis and characterization of Al_2O_3–CeO_2 composite nanopowder, J. Alloys Compd. 494 (2010) 289–294.
[3] D.N. Nhiem, L.M. Dai, N.D. Van, D.T. Lim, Catalytic oxidation of carbon monoxide over nanostructured CeO_2–Al_2O_3 prepared by combustion method using polyvinyl alcohol, Ceram. Int. 39 (2013) 3381–3385.
[4] Y. Huang, Y. Cai, D. Qiao, H. Liu, Morphology-controllable synthesis and characterization of CeO_2 nanocrystals, Particuology 9 (2011) 170–173.
[5] S. Supakanapitak, V. Boonamnuayvitaya, S. Jarudilokkul, Synthesis of nanocrystalline CeO_2 particles by different emulsion methods, Mater. Charact. 67 (2012) 83–92.
[6] A. Hadi, I.I. Yaacob, Novel synthesis of nanocrystalline CeO_2 by mechanochemical and water-in-oil microemulsion methods, Mater. Lett. 61 (2007) 93–96.
[7] S.A. Hassanzadeh-Tabrizi, E. Taheri-Nassaj, Synthesis of high surface area Al_2O_3–CeO_2 composite nanopowder via inverse co-precipitation method, Ceram. Int. 37 (2011) 1251–1257.
[8] R. Ebrahimi-Kahrizsangi, O. Torabi, Combination of mechanochemical activation and self-propagating behavior for the synthesis of nanocomposite Al_2O_3/B_4C powder, J. Alloys Compd. 514 (2012) 54–59.
[9] G. Mouret, K. Mozet, H. Muhr, E. Plasari, M. Martin, Production of Al_2O_3–TiO_2 catalyst supports with controlled properties using a co-precipitation process, Powder Technol. 190 (2009) 84–88.
[10] M.A. Ahmed, M.F. Abdel-Messih, Structural and nano-composite features of TiO_2–Al_2O_3 powders prepared by sol–gel method, J. Alloys Compd. 509 (2011) 2154–2159.
[11] A.I.Y. Tok, F.Y.C. Boey, Z. Dong, X.L. Sun, Hydrothermal synthesis of CeO_2 nano-particles, J. Mater. Process. Technol. 190 (2007) 217–222.
[12] K.-l. Huang, L.-g. Yin, S.-q. Liu, C.-j. Li, Preparation and formation mechanism of Al_2O_3 nanoparticles by reverse microemulsion, Trans. Nonferrous Met. Soc. China 17 (2007) 633–637.
[13] M.A. Malik, M.Y. Wani, M.A. Hashim, Microemulsion method: a novel route to synthesize organic and inorganic nanomaterials: 1st nano update, Arabian J. Chem. 5 (2012) 397–417.
[14] G.C. Bond, Heterogeneous Catalysis: Principles and Applications, Oxford Science Publication, Oxford, UK, 1987.
[15] L. Hu, Z. Tang, Z. Zhang, Template-assisted synthesis of mesoporous $LiAlO_2$ hollow spheres with high surface area, Microporous Mesoporous Mater. 113 (2008) 41–46.
[16] S.A. Hassanzadeh-Tabrizi, Optimization of the synthesis parameters of high surface area ceria nanopowder prepared by surfactant assisted precipitation method, Appl. Surf. Sci. 257 (2011) 10595–10600.
[17] S. Eriksson, U. Nyle´n, S. Rojas, M. Boutonnet, Preparation of catalysts from microemulsions and their applications in heterogeneous catalysis, Appl. Catal. A: Gen. 265 (2004) 207–215.
[18] F.C. Meldrum, N.A. Kotov, J.H. Fendler, Preparation of particulate monolayers and multilayers from surfactant-stabilized, nanosized magnetite crystallites, J. Phys. Chem. 98 (1994) 4506–4510.